Biological Trace Element Research (2024) 202:3714–3730
https://doi.org/10.1007/s12011-023-03955-y

RESEARCH

Pancreatic Antioxidative Defense and Heat Shock Proteins Prevent Islet of Langerhans Cell Death After Chronic Oral Exposure to Cadmium LOAEL Dose

Diana Moroni-González[1] · Victor Enrique Sarmiento-Ortega[1] · Alfonso Diaz[2] · Eduardo Brambila[1] · Samuel Treviño[1]

Received: 12 August 2023 / Accepted: 6 November 2023 / Published online: 13 November 2023

Abstract

Cadmium, a hazardous environmental contaminant, is associated with metabolic disease development. The dose with the lowest observable adverse effect level (LOAEL) has not been studied, focusing on its effect on the pancreas. We aimed to evaluate the pancreatic redox balance and heat shock protein (HSP) expression in islets of Langerhans of male Wistar rats chronically exposed to Cd LOAEL doses, linked to their survival. Male Wistar rats were separated into control and cadmium groups (drinking water with 32.5 ppm $CdCl_2$). At 2, 3, and 4 months, glucose, insulin, and cadmium were measured in serum; cadmium and insulin were quantified in isolated islets of Langerhans; and redox balance was analyzed in the pancreas. Immunoreactivity analysis of p-HSF1, HSP70, HSP90, caspase 3 and 9, and cell survival was performed. The results showed that cadmium exposure causes a serum increase and accumulation of the metal in the pancreas and islets of Langerhans, hyperglycemia, and hyperinsulinemia, associated with high insulin production. Cd-exposed groups presented high levels of reactive oxygen species and lipid peroxidation. An augment in MT and GSH concentrations with the increased enzymatic activity of the glutathione system, catalase, and superoxide dismutase maintained a favorable redox environment. Additionally, islets of Langerhans showed a high immunoreactivity of HSPs and minimal immunoreactivity to caspase associated with a high survival rate of Langerhans islet cells. In conclusion, antioxidative and HSP pancreatic defense avoids cell death associated with Cd accumulation in chronic conditions; however, this could provoke oversynthesis and insulin release, which is a sign of insulin resistance.

Keywords Cadmium · Oxidative stress · Heat shock proteins · Langerhans islets · Pancreas

Introduction

In recent years, epidemiological studies have demonstrated that environmental exposures to low levels of toxic metals associated with deficient intakes of essential metals through food give rise to diverse pathologies. Particularly, cadmium (Cd) is a non-essential transition metal, considered one of the top five most hazardous environmental contaminants by the Agency for Toxic Substances and Disease Registry (ATSDR) [1]. Even in very low concentrations, Cd poses a significant health risk because it is poorly excreted and cannot undergo degradation or biotransformation to less toxic species [2]. The ATSDR has defined a minimal risk level of Cd exposure based on daily exposure to metal that is likely to be without an appreciable risk of adverse effects, such as cancer development. From the minimal risk level, two levels or doses of adverse effects have been established for oral Cd consumption: no observable adverse effect level (NOAEL) and lowest observable adverse effect level (LOAEL) [1]. The LOAEL dose in the range of 1 µg to 2 mg of Cd/day, depending on duration time and toxicokinetic of the metal, represents a significant health hazard to the world population because it is associated with nephrotoxicity, neurotoxicity, endocrine and reproductive defects, and developing

✉ Samuel Treviño
samuel.trevino@correo.buap.mx

[1] Laboratory of Chemical-Clinical Investigations, Department of Clinical Chemistry, Chemistry Department, Meritorious Autonomous University of Puebla, 14 Sur. FCQ1, Ciudad Universitaria, 72560 Puebla, C.P, Mexico

[2] Department of Pharmacy, Faculty of Chemistry Science, Meritorious Autonomous University of Puebla, 22 South, FCQ9, Ciudad Universitaria, 72560 Puebla, C.P, Mexico

steatosis, metabolic syndrome, atherogenesis, prediabetes, and type 2 diabetes (T2D) [3–8].

Evidence suggests that although chronic exposure to Cd LOAEL in drinking water has been associated with an increased risk for developing dysglycemia and T2D, it is not related to the death of β-cells [6, 9]. However, Cd accumulation has been detected in the pancreas [6]. The β-cell can adapt in response to insults and insulin demand. In increased insulin demands such as hyperglycemia, β-cells increase insulin biosynthesis or compensate via hypertrophy and hyperplasia. Cd exposure increases some biomarkers related to β-cell hypertrophy and hyperplasia. Additionally, mass β-cell preservation (regarding the integrity of the architecture, structure, number, cell size, and function) is crucial to prevent the development of T2D [10]. Due to β-cells being susceptible to uncontrolled distress caused by inflammation, reactive oxygen, and nitrogen species (ROS and RNS), the protective and antioxidant β-cell defense must respond precisely [11].

The pancreatic defense comprises vitamins (e.g., C and E), peptides, and proteins, such as metallothionein (MT) and glutathione (GSH), as well as enzymes such as superoxide dismutase (SOD), catalase (CAT), γ-glutamyl cysteine synthetase, GSH peroxidase (GPx), GSH reductase (GR), and GSH transferase (GST), that minimize oxidative damage [12–14]. However, the pancreatic antioxidant defense has a low threshold compared with other tissues, such as the liver, heart, or muscles. Therefore, other molecules must strengthen the β-cell defense, such as heat shock proteins (HSP), which is an effective defense mechanism in response to Cd exposure [10, 15–17].

HSP70 family members are indicators of oxidative stress with high sensitivity to dysregulations of oxidative responses in different mammalian cells, especially in β-cell disorders [18]. HSP90 was initially recognized as a stress-induced protein [19]. Recently, it has been shown that HSP90 forms molecular chaperone complexes, which protect the endoplasmic reticulum and mitochondria against β-cell stressors as reviewed in [17, 20]. However, HSP has not been studied in β-cells chronically exposed to Cd. Therefore, we aimed to evaluate the harmful effects of Cd on pancreatic redox and β-cell defense mechanisms of male Wistar rats chronically exposed to Cd LOAEL dosage as a possible link to metabolic imbalance.

Material and Methods

Animals and Treatment

One hundred twenty male Wistar rats (1 month of age) were obtained from the "Claude Bernard" Animal Facility of the University of Puebla, Mexico. The rats were housed in acrylic boxes at controlled temperature and humidity, with light-dark cycles of 12 h each, with free access to water and food. The diet used was LabDiet 5001 (Laboratory Rodent Diet). The rats were divided randomly into the control group (LabDiet 5001 + water free of Cd, *ad libitum*, $n = 45$ rats) and the Cd-exposed group (LabDiet 5001 + drinking water with 32.5 ppm of $CdCl_2$, ad libitum, $n = 75$ rats). Cadmium exposure at the LOAEL dose (32.5 ppm of $CdCl_2$) was performed for 2, 3, and 4 months ($n = 25$ for each subgroup) [5, 7]. Weight and daily water consumption were monitored (Fig. Supplementary 1). Rats consumed a mean of 1.99 mg Cd/100 g/day during Cd exposure, considering the average water consumption and weight of each rat.

Control and Cd groups were processed under the same conditions. The pancreas was obtained after a pentobarbital dose (intraperitoneally) in each experimental time cohort. After the excision, the pancreas was thoroughly perfused with cold Hank's buffer salt solution (HBSS) and dissected, taking the pancreatic duct as a reference. The up section was stored at − 70 °C (for cadmium and redox balance), while the lower section was fixed in neutral buffered formalin (4%) for histology analysis. The procedures described in this study were performed following the Standards for the Use and Care of Laboratory Animals described by the Mexican Council for Animal Care (NOM-062-ZOO-1999), as well as the Guide of the National Institutes of Health for the Care and Use of Laboratory Animals, and the Ethics Committee of the Autonomous University of Puebla. All applicable international, national, and institutional guidelines for the care and use of animals were followed to minimize possible discomfort.

Insulin and Glucose Serum Assays

Whole blood samples were obtained by direct cardiac puncture in dead animals, and after centrifugation, serum was used to perform insulin and glucose analysis. The serum concentrations of glucose were determined using an A15 autoanalyzer (BioSystems, Guadalajara, Mex.), and serum insulin was quantified by ELISA in a Stat fax 2600 plate reader at 415 nm (WinerLab Group, Buenos Aires, Argentina).

Islet Isolation

After euthanasia, five rats per group were given an abdominal incision aseptically; the common bile duct was cannulated with a 27-gauge needle, and the pancreas was distended with 5 mL of cold HBSS and 2 mg/mL collagenase type V (C9263, Sigma Aldrich, Mexico). The pancreas was collected, and collagenase digestion (2 mg/mL in HBSS) was performed in a water bath at 37 °C. After 9 min, the digestion was stopped with 10 mL of cold HBSS mixing for

1 min. Then, 40 mL of cold HBSS was added and centrifuged for 2:30 min at 290 *g*. The supernatant was discarded, and the pellet was resuspended with 10 mL of cold HBSS. Undigested tissue was separated with 10 mL of cold HBSS. Afterward, it was centrifuged for 3:00 at 290 *g*. The supernatant was discarded again, the pellet was resuspended in 5 mL of Histopaque 1.119, and 5 mL of Histopaque 1.077 was carefully added (Sigma Aldrich, Mexico). On the top, 10 mL of cold HBSS was added and centrifuged at 900 *g* for 20 min to separate acinar from islet cells. Purified islets were manually counted under light microscopy [21].

Pancreatic Insulin Quantification

From 100 Langerhans islets, insulin was extracted with acid-alcohol at 4 °C overnight. It was centrifuged at 500 *g* and 4 °C. Supernatant was placed in a 15-mL conical tube and stored at −20 °C until analysis. The amount suggested by the ELISA immunoassay manufacturer was taken from the supernatant, and the indications of the working kit were followed. The antigen-antibody complex was measured at a wavelength of 415 nm in an automated Stat fax 2600 reader (WinerLab Group, Buenos Aires, Argentina).

Cadmium Quantification

Cadmium concentration was determined using an inductively coupled plasma optical emission spectrometer (Mod. 730-ES, Varian Inc., USA). Serum samples were digested with a solution of nitric acid (65%, Sigma Aldrich, Mexico) and hydrochloric acid (30%, Sigma Aldrich, Mexico) in a 1:1 ratio [22]. Meanwhile, 200 mg of pancreas tissue and 50 mg of islets of Langerhans were separately placed in nitric acid (50%) and perchloric acid (15.6 M) solution in a 1:1 ratio. The mixture was incubated at 37 °C for 3 days in an ACCU BLOCJTM bath (Labnet International, USA) until complete digestion. Then, each sample was diluted with deionized water to a final volume of 3 mL. Deionized water (resistivity 18.2 MΩ cm) was dispensed from a Barnstead Easypure II water system (Thermo Fisher Scientific, Marietta, OH, USA). Equipment calibration was performed using two tuning solutions: mixed stock and internal standards. Six-point calibration standards at suitable ranges were generated. Certified tuning, mixed stock standard, and internal standard solutions were acquired from Agilent Technologies (Santa Clara, CA, USA) [4]. Cadmium in pancreatic tissue was adjusted to grams of tissue, while Cd in islets of Langerhans was adjusted to mg of protein.

Histology

After formalin fixation, pancreatic tissue was placed in an automatic tissue processor (Leica TP1020, Wetzlar, Germany) for dehydration, clarification, infiltration, and inclusion in paraffin blocks (Paraplast, Leica, Mexico). Tissue sections 5-µm thick were taken from each tissue. Paraffin was removed, and the tissues were rehydrated.

Insulin Immunohistochemistry

Pancreatic sections were processed for antigen retrieval and endogenous peroxidase inactivation and then incubated in 2% IgG-free bovine serum albumin (BSA, Sigma Aldrich, Mexico) to block non-specific binding sites. Then, the samples were permeated with 0.2% Triton X-100, washed with phosphate-buffered solution (PBS), and subsequently incubated overnight at 4 °C with primary antibody (1:250; ab7842, Abcam, Mexico). At the end of the incubation, the samples were washed with PBS. Peroxidase-conjugated secondary antibody (1:500; ab6908, Abcam, Mexico) was incubated for 2 h at room temperature, finally washed with PBS, and they were revealed with 3,3′-diaminobenzidine. Photomicrographs magnified 400× were obtained using a bright-field microscope attached to a camera (Leica Microsystems GmbH, Wetzlar, Germany).

Immunofluorescence Assays

Immunofluorescence assays were performed. Tissue sections after antigen retrieval and non-specific binding sites were blocked with bovine serum albumin (2% IgG-free) and incubated with primary antibodies: HSP70 (Sc-24), HSP90 (Sc-11139), phosphorylated heat shock factor 1 (p-HIF1; Sc-17757), caspase 3 (Sc-7272), and caspase 9 (Sc-73548) were incubated overnight at 4 °C in a dark room, at the end of incubation, sections were washed with PBS, and Rhodamine or FICT-conjugated secondary antibody, as appropriate, was incubated for 2 h at room temperature (Santa Cruz Biotechnology, Inc., Dallas, Texas, USA). Finally, a vectashield mounting medium with DAPI was placed for nuclei identification and tissue sections were sealed (Vector Laboratories, Newark, California, United States).

Photomicrographs were taken in a fluorescence microscope (Leica Microsystems GmbH, Wetzlar, Germany) and projected with a Leica IM1000 version 1.20 release-9 computer-based program (Imagic Bildverarbeitung AG, Leica Microsystems, Heerbrugg, Switzerland). The semi-quantitative immunofluorescence was performed, establishing a continuous scale of pixel intensity per unit area for red or green channels independently with positive and negative samples. Graphical constructions for each mark were performed in the ImageJ program version 1.53 bundled with 64-bit Java 8 for Windows (National Institute of Health, USA). Then, the area of the islets of Langerhans was delimited, and pixel intensity was measured, which was represented as optic density (OD) in arbitrary units (AU).

Viability Assay

A viability assay was performed by acridine orange (AO) staining. A work solution was prepared with 2 mg/mL AO in distilled water diluted to 1:100 with a 10 mM citrate-phosphate buffer, 0.1M NaCl at pH 3.8 (to 150 mL of distilled water added 9.92 mL of 0.1 M citric acid, 5.46 mL 0.2 M of dibasic sodium phosphate, and 1.7g of NaCl). Then, to rehydrate tissue sections, 0.5 mL of buffer was used: 20 mM of citrate-phosphate, 0.1 mM of EDTA, 0.2 M of sucrose, and 0.1% of Triton X-100, at room temperature, pH 3.0, and agitation for 5 min. Afterward, the slides were washed and covered with the previously prepared work solution, and they were agitated for 5 min at room temperature. Finally, tissues were washed with PBS, dried, 50 µL of vectashield was placed, and the tissues were sealed. AO interacts with DNA and RNA by intercalation or electrostatic attraction, respectively. DNA intercalated with AO fluoresces green (525 nm; viable cells); RNA or denaturalized DNA has electrostatically bound AO, emitting fluorescent red (>630 nm; apoptotic cells). The viability was evaluated using a fluorescence microscope attached to a camera (Leica Microsystems GmbH, Wetzlar, Germany). Cell count was performed with the ImageJ program version 1.53 bundled with 64-bit Java 8 for Windows in independent channels. The cell count was represented as a viability percentage in each islet of Langerhans ($n = 100$). All reagents used were acquired from Sigma Aldrich (Sigma Aldrich, Mexico).

The Quantification of Total Proteins

From biopsies, 100 mg of tissue was homogenized in 800 µL of SSI. Quantifying total proteins was performed using the Sedmak and Grossberg method and a standard curve of bovine serum albumin [23]. The proteins were quantified in 1 µL of the homogenate supernatant plus 500 µL of the color reagent (Coomassie blue 0.06%), taking it to 1 mL with distilled water. All parameters were adjusted to the total protein content of the sample (mg of protein).

Lipid Peroxidation

Lipid peroxidation products, malondialdehyde (MDA), and 4-hydroxyalkenals (4HDA) were measured in the supernatants of pancreas homogenates [24]. The colorimetric reaction was performed using 200 µL of supernatant after the subsequent addition of 650 µL of 10.3 mM N-methyl-2-phenyl-indole was diluted in a mixture of acetonitrile to methanol (3:1) and 150 µL of methanesulfonic acid or hydrochloric acid, respectively. The reaction mixture was vortexed and incubated at 45 °C for 1 h and centrifuged at 550 *g* for 10 min. The absorbance in the supernatant was read at 586 nm with a SmartSpec 3000 spectrophotometer (Bio-Rad, Hercules, CA, USA). The absorbance values were compared to a standard curve in the concentration range of 0.5 to 5 µM of 1,1,3,3-tetramethoxypropane (10 mM stock) to calculate the malondialdehyde + 4-hydroxyalkenal (MDA + 4HDA) in the samples.

Nitrite Assay

The nitrites were measured using the Griess reaction [25]. The Griess reagent had equal volumes of 0.1% N-(1-naphthyl) ethylenediamine dihydrochloride and 1.32% sulfanilamide in 60% acetic acid (Sigma Aldrich, Mexico). The colorimetric reaction was made in 100 µL supernatant and 100 µL Griess reagent. The absorbance of the samples was determined at 540 nm in a spectrophotometer and compared to a standard curve of $NaNO_2$ in each assay. Results were expressed as micromoles of nitrite per milligram of protein (µM of NO_2^-/mg of protein).

Reactive Oxygen Species Quantification

Intracellular ROS levels were measured with fluorometry. Five microliters of supernatant was diluted in 9 vol. of 40 mM TRIS plus HEPES buffer and then incubated with 5 µM of 2′7′-dichlorodihydrofluorescein diacetate (DCFH-DA). The samples were incubated for 1 h at 37 °C under constant shaking before the fluorescence signals were determined in a PerkinElmer LS50-B luminescence spectrometer at 488 nm excitation and 525 nm emission wavelengths. Values were obtained by interpolating the readings with a 2′7′-dichlorofluorescein (DCF) standard curve (Sigma Aldrich, Mexico) [4].

Glutathione System and Metallothionein Quantification

The metallothionein (MT) concentration was determined by the saturation method with ^{109}Cd [26]. Meanwhile, the enzymatic recycling technique based on glutathione reductase determined glutathione content in biological samples. Glutathione is oxidized by 5,5′-2-nitrobenzoic acid (DTNB) to form the yellow derivative 5′-thio-2-nitrobenzoic acid, measurable at 412 nm. The glutathione disulfide (GSSG) formed can be recycled to GSH by glutathione reductase in the presence of NADPH [27]. For the calculation of the GSH concentration, the following operation was performed: GSH = total glutathione − GSSG. The following operation, Ind Redox = 2GSH/GSSG, was used to calculate the redox index.

Glutathione peroxidase (GPx) activity was quantified as described by Flohé and Günzler [28]. The GPx in the supernatant reduces the hydroperoxides to the tert-butyl hydrogen peroxide substrate, and the enzyme is oxidized.

The oxidized GPx is regenerated by GSH, which is oxidized to GSSG. GSSG returns to GSH by donating an electron from NADPH via glutathione reductase (GR). The rate of NADPH decrease is directly proportional to the activity of GPx, which was measured spectrophotometrically at 340 nm (PerkinElmer Lambda EZ-150). The measured activity was expressed in µmol/min/mg of protein.

Glutathione S-transferase (GST) activity was determined using the method described by Habig [29]. The work solution is a mix: 33 mM of HEPES buffer at pH 7.5, 1.5 mM GSH, 1.5 mM of 1-chloro-2-dinitrobenzene (CDNB), and water in a final volume of 1 mL. The conjugation of GSH with CDNB in the presence of GST measures its activity, which can be followed spectrophotometrically at 340 nm for 3 min. The activity was reported as µmol/min/mg of protein.

Glutathione reductase (GR) activity was determined by monitoring the oxidation of NADPH in the presence of GSSG according to the method of Smith et al. [30]. The GSH formed reacts with DTNB, showing an increase in absorbance measured at 412 nm. The reaction system contained 0.1 M phosphate buffer (pH 7.5), 1 mM EDTA, 2 mM GSSH, and 3 mM DTNB solution. The addition of 2 mM NADPH started the reaction.

Catalase and Superoxide Dismutase Activity Assay

The catalase activity (CAT) was quantified using ultraviolet light spectrophotometry. The homogenates (0.05 mL) were mixed with 2.0 mL of potassium phosphate buffer (50 mM at pH 7.0) and 0.05 mL of H_2O_2 (0.3 M). Absorbance followed for 60 s at 240 nm. The catalase activity was calculated as µmol/min/mg of protein equal to U/mg of protein [31].

Superoxide dismutase (SOD) was analyzed using the pyrogallol method. The superoxide radical is generated by pyrogallol auto-oxidation, absorbing the light at 420 nm. The presence of SOD inhibits autoxidation by preventing propagation reactions. By agreement, 1 U of SOD is taken as the amount of enzyme that inhibits the auto-oxidation reaction of pyrogallol by 50% at 25 °C and pH 8.2 [4].

Statistical Analysis

A Shapiro-Wilk normality test was performed to verify that the different data come from a normally distributed population. The results were expressed as the mean ± SEM for all experiments. The Student *t*-test analyzed parametric variables. The Mann–Whitney *U* test was used for non-parametric tests. The supplementary results were analyzed by a two-way ANOVA followed by a Bonferroni test. Data analysis was performed with GraphPad Prism 8 (GraphPad Software Inc., USA). Asterisk (*) indicates statistical differences between control and experimental groups in each time cohort. The significance level was set at $p \leq 0.05$.

Results

Monitoring of Water Consumption and Weight

The weight of animals exposed to cadmium was significantly lower ($p = 0.004$) at two months (310.8 + 8.2 g) regarding non-exposed rats (341.8 + 7.2 g). However, at 3 and 4 months, the groups were not statistically different; thereby, the interaction between variables time and treatment was low ($F = 12.3$). Likewise, the variables of time and water consumption were analyzed. The results showed that the Cd group consumed more water than non-exposed rats, and at three months, it was statistically different ($p = 0.002$), and important interaction between variables was observed ($F = 58.7$). Finally, the interaction between the weight and water consumption was analyzed; the results showed a strong interaction ($F = 135.6$), where rats with Cd exposed with a less weight consumed more water than the control groups, which could be related to intestinal Cd absorption and its accumulation in the pancreas (Fig. S1).

LOAEL Dose Generates Serum Increase, Islets of Langerhans, and the Pancreatic Accumulation of Cadmium

LOAEL dosage produced a serum increase of cadmium in the chronically exposed groups, from 3.8 µg/L (2 months) to 5.5 µg/L (4 months). In the pancreas, Cd accumulated from 1.9 to 3.9 µg/g of tissue over time. Meanwhile, a similar behavior was observed in the islets of Langerhans; the Cd levels were from 0.25 to 0.55 µg/mg of protein over time (Fig. 1A–C).

Chronic Cadmium Exposure Causes Hyperglycemia, Hyperinsulinemia, and Overinsulin Storage

Fasting hyperglycemia was observed in Cd-exposed rats, evidencing a significant increase of 85% (2 months), 70.5% (3 months), and 78.4% (4 months). Meanwhile, fasting hyperinsulinemia also increased in Cd-exposed rats at 2 (76%), 3 (95%), and 4 months (55%) (Table 1). Additionally, the insulin content in islets of Langerhans was quantified. A significant increase was observed at 2 (30%), 3 (19%), and 4 months (10%; Fig. 2G) in Cd-exposed rats regarding control groups. The results were corroborated by histochemistry, where a significant insulin immunoreactivity was observed in the islets of Langerhans of Cd-exposed groups (Fig. 2D–F).

Chronic Cadmium Exposure and Pancreatic Redox Balance

We quantified the oxidative status after verifying that insulin and Cd are overstored in islets of Langerhans. ROS

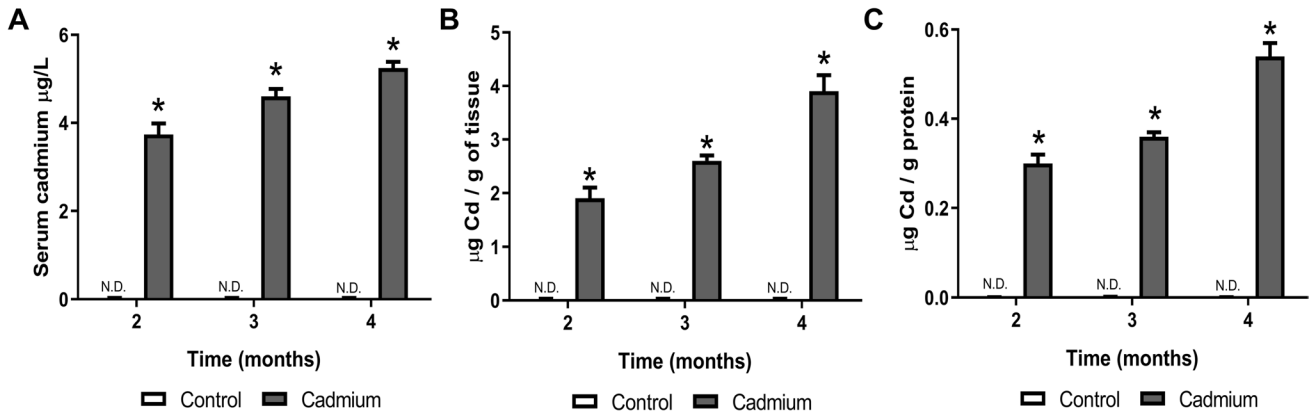

Fig. 1 Serum and pancreatic tissue cadmium accumulation. The metal was quantified by inductively coupled plasma optical emission spectrometry. **A** Cd serum concentration. **B** Cd pancreas concentration. **C** Cd islets of Langerhans concentration in control and Cd-exposed groups at 2, 3, and 4 months. The data presented are the mean of the measured values ± the SEM (standard error of the mean). For serum and pancreas assays, $n = 10$ for controls and $n = 20$ for cadmium groups. Meanwhile, for Cd islets of Langerhans concentration, $n = 5$ for controls and cadmium groups. *Significant difference from the control group ($p \leq 0.05$ by Student's *t*-test). Cd quantification was performed from the total pancreas and isolated islets digested

Table 1 Serum glucose and insulin

	2 months		3 months		4 months	
	Control	Cadmium	Control	Cadmium	Control	Cadmium
n	15	25	15	25	15	25
Glucose (mg/dL)	90.1 ± 4.4	166.6 ± 14*	94.4 ± 3.8	160.9 ± 23.1*	93.6 ± 4.9	167.0 ± 16.2*
Insulin (µUI/mL)	11.7 ± 0.7	20.6 ± 0.9*	10.2 ± 0.4	19.9 ± 0.5*	9.3 ± 0.7	14.4 ± 0.4*

The data are the mean of the values ± SEM (standard error of the mean)

*Significant difference from the control group ($p \leq 0.05$ by Student's *t*-test)

concentration significantly increased by 210% (3rd month) and 258% (4th month) in Cd-exposed rats (Fig. 3A). However, nitrite concentration was not different between exposed and non-exposed groups (Fig. 3B). Meanwhile, 4HDA and MDA (Fig. 3C, D) concentrations significantly increased at 2 months (264% and 237%), 3 months (174% and 251%), and 4 months (150% and 236%).

In Cd-exposed groups, the MT concentration increased by 170%, 220%, and 205%; total glutathione increased by 65%, 75%, and 54%; and the reduced fraction (GSH), which is what provides cell protection, also increased by 50%, 57%, and 54%, respectively, in each time cohort. Although glutathione oxidized fraction (GSSG) also increased by 50% and 60% in the 3rd and 4th months in Cd-exposed animals, the redox index showed an antioxidant environment because it was higher by 33% and 21% during 2 and 3 months of analysis (Table 2).

The activity of the enzyme glutathione system was also measured. The results showed that GST activity increased by 33% (3 months) and 74% (4 months) in Cd-exposed rats; the GR activity diminished by 24% in the fourth month. The GPx activity showed a dual behavior, increasing by 35% at 2 months of Cd exposure, while in the fourth month, it decreased by 41%, regarding the control group. Additionally, SOD and CAT activity increased at 2 (108% and 75%), 3 (62.5% and 90%), and 4 months (142% and 133%; Table 2).

Chronic Cadmium Exposure Increases HSP Expression

The HSP response is essential to maintain cell viability, and their transcriptional regulation is in charge of HSF1. We analyzed the immunoreactivity of the active HSF1 form. The result showed a significant increase of 221%, 242%, and 365% in a time-dependent manner in Cd-exposed groups (Fig. 4D–G). In the same way, the HSP70 and 90 immunoreactivities increased at 2 (79% and 132%), 3 (259% and 225%), and 4 months (92% and 227%) in Cd-exposed groups (Figs. 5 and 6D–G).

Chronic Cadmium Exposure and Islets of Langerhans Viability

We analyzed caspase expression and cell viability to investigate whether oxidative status and cadmium accumulation induce cell death in islets of Langerhans. The

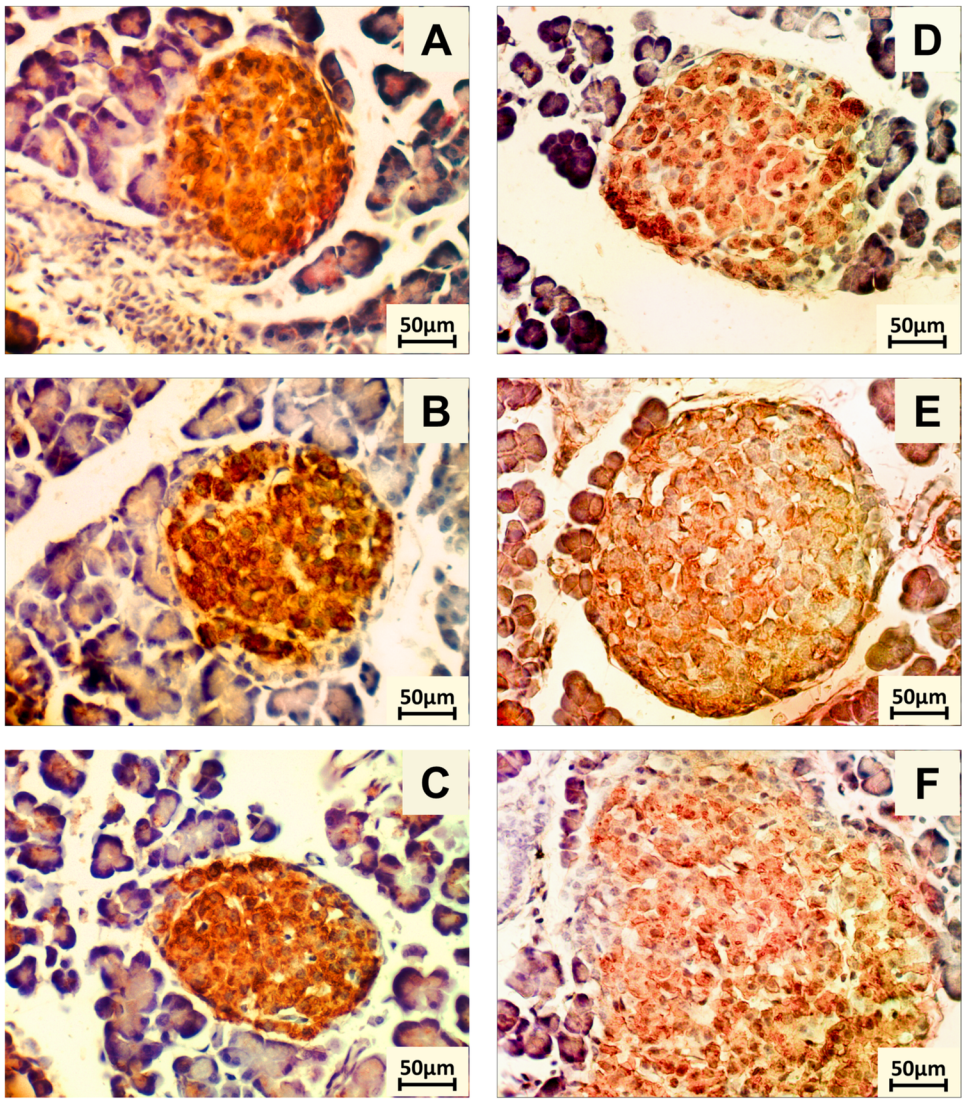

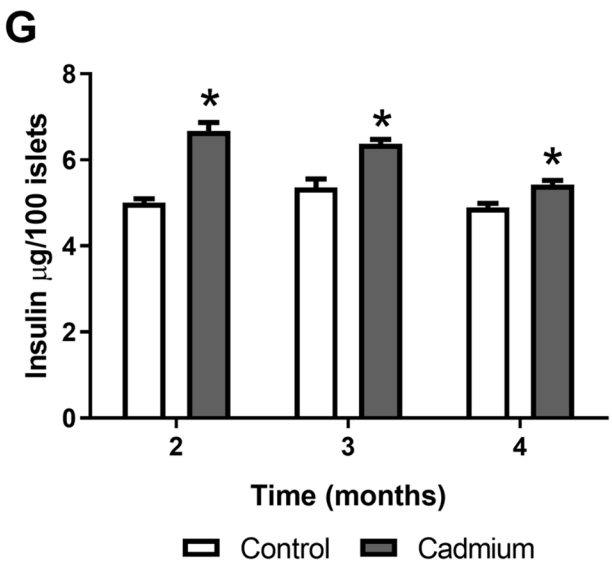

Fig. 2 Insulin Production. **A–C** Representative photomicrographs of the control groups of 2, 3, and 4 months are shown with a 40× objective ($n = 100$, islets analyzed). **D–F** Representative photomicrographs of Cd-exposed groups for 2, 3, and 4 months are shown with a 40× objective ($n = 100$, islets analyzed). **G** Quantification of insulin. The data presented are the mean of the measured values ± the SEM (standard error of the mean). For immunohistochemistry assays, $n = 10$ for controls and $n = 20$ for cadmium groups. Meanwhile, $n = 5$ for controls and cadmium groups for insulin assay. *Significant difference from the control group ($p \leq 0.05$ by Student's *t*-test). Insulin quantification was performed from isolated islets

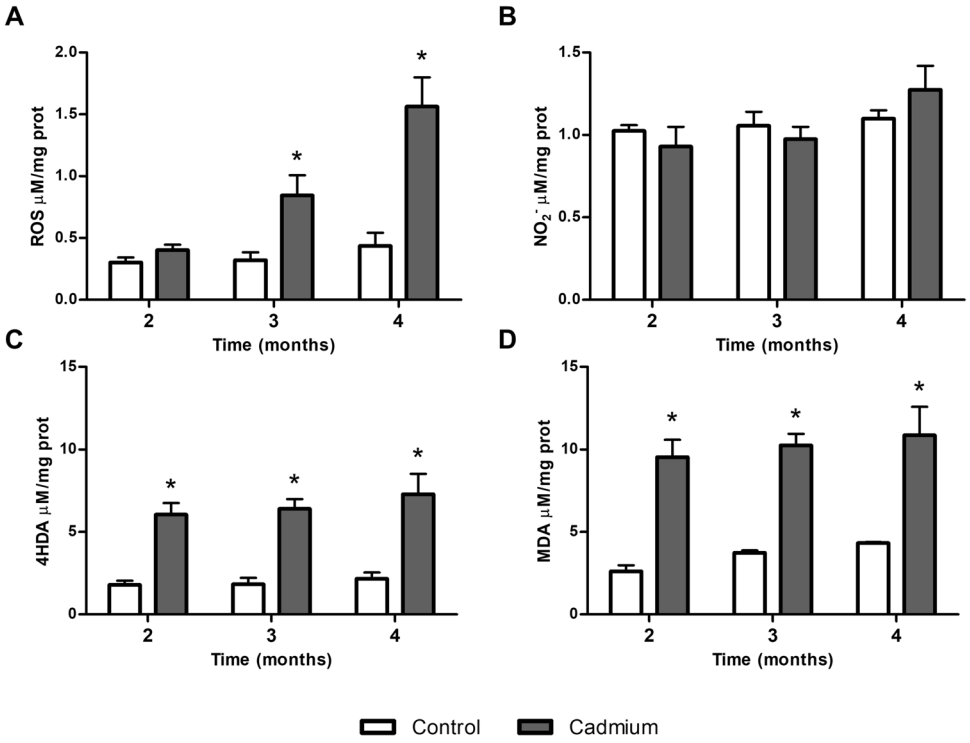

Fig. 3 Pancreatic oxidative status. **A** ROS. **B** NO_2^-. **C** MDA. **D** 4HDA. The data presented are the mean of the measured values ± the SEM (standard error of the mean) performed in triplicate, $n = 10$ for controls and $n = 20$ for cadmium groups. *Significant difference from the control group ($p \leq 0.05$ by Student's *t*-test). The measurements were performed from the pancreas lysate

Table 2 Pancreatic antioxidant defense

	2 months		3 months		4 months	
	Control	Cadmium	Control	Cadmium	Control	Cadmium
n	10	20	10	20	10	20
Total glutathione (µM/mg of Prot)	0.92 ± 0.17	1.51 ± 0.22*	0.9 ± 0.13	1.57 ± 0.13*	1.33 ± 0.18	2.05 ± 0.13*
GSH (µM/mg of Prot)	0.88 ± 0.2	1.46 ± 0.22*	0.86 ± 0.4	1.51 ± 0.14*	1.27 ± 0.19	1.97 ± 0.13*
GSSG (µM/mg of Prot)	0.04 ± 0.005	0.05 ± 0.006	0.04 ± 0.006	0.06 ± 0.006*	0.05 ± 0.008	0.08 ± 0.005*
2GSH/GSSG	42 ± 2.7	56 ± 2.4*	40.3 ± 4.0	48.7 ± 1.6*	48.1 ± 2.1	48.2 ± 1.4
GPx nmol min^{-1}/mg of Prot	13.7 ± 1.5	18.5 ± 1.4*	13.5 ± 1.2	11.1 ± 1.2	13.3 ± 1.4	7.9 ± 1.1*
GR mU min^{-1}/mg of Prot	193.5 ± 15	196 ± 12.5	191.7 ± 14.3	213.8 ± 15	192.1 ± 14.2	147.3 ± 12.4*
GST U min^{-1}/mg of Prot	179.6 ± 15	208.8 ± 15	181.3 ± 11.9	241.4 ± 17*	188.1 ± 16	327.9 ± 23*
SOD U min^{-1}/mg of Prot	4.8 ± 0.7	10 ± 1.42*	7.2 ± 0.81	11.7 ± 1.43*	7.8 ± 0.7	18.9 ± 2.5*
CAT U min^{-1}/mg of Prot	13 ± 0.8	22.8 ± 2.47*	16.1 ± 1.82	30.7 ± 3.9*	20.2 ± 2.4	47.1 ± 4*
MT µg/g of tissue	1.19 ± 0.3	3.22 ± 0.4*	1.01 ± 0.2	3.34 ± 3.9*	1.18 ± 0.2	3.6 ± 0.2*

The data presented are the mean of the measured values ± the SEM (standard error of the mean). The measurements were performed from pancreas lysates

GSH reduced glutathione, *GSSG* oxidized glutathione, *2GSH/GSSG* oxidative ratio, *GPx* glutathione peroxidase, *GR* glutathione reductase, *GST* glutathione S-transferase, *SOD* superoxide dismutase, *CAT* catalase, *MT* metallothionein

*Significant difference from the control group ($p \leq 0.05$ by Student's *t*-test)

normalized immunoreactivity for caspases 3 and 9 did not differ between Cd-exposed and non-exposed groups in the analyzed times (Fig. 7A, C, D). Islets of Langerhans of animals that were non-exposed to cadmium presented a viability close to 95%, while the Cd-exposed groups had a viability between 80% during analyzed times (Fig. 7A, B).

Discussion

Herein, we investigated whether protective pancreatic cell defense can prevent the detrimental effects and cell death caused by chronic oral exposure to cadmium LOAEL dose

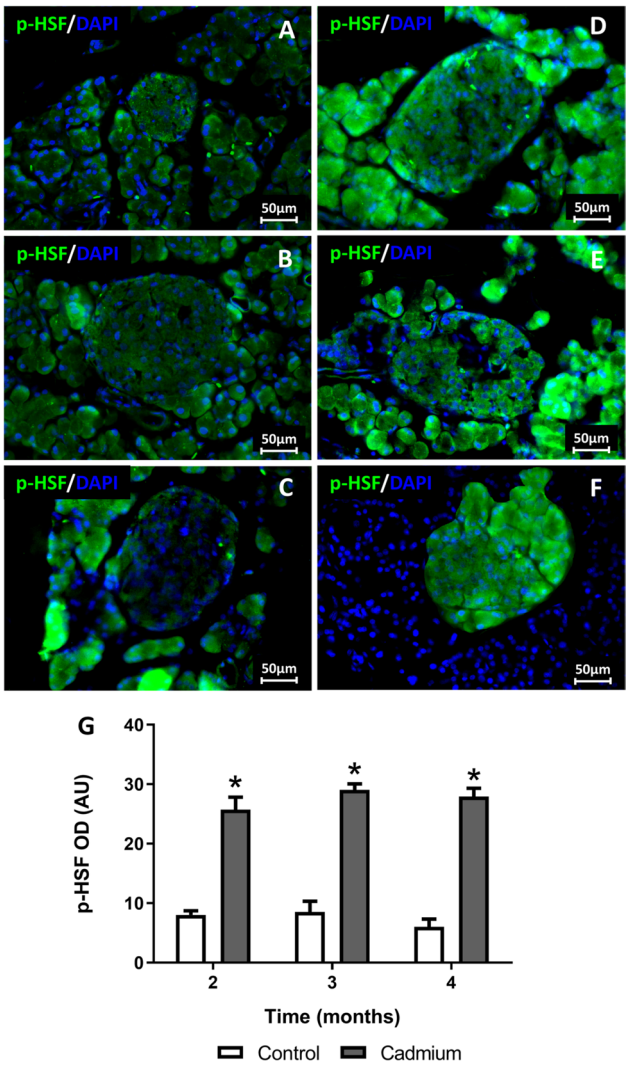

Fig. 4 Heat shock factor 1 analysis. **A–C** Representative photomicrographs of the control groups of 2, 3, and 4 months (n = 100 islets; 40× objective). **D–F** Representative photomicrographs of Cd-exposed groups at 2, 3, and 4 months (n = 100 islets; 40× objective). **G** Semi-quantitative analysis of the immunoreactivity to HSF1. *Significant difference from the control group ($p \leq 0.05$ by Mann–Whitney U test). The analysis was performed from the pancreas lysate

of 32.5 ppm in drinking water. Cadmium reduced the weight of exposed rats to metal. Still, it did not affect the volume of water consumption, which has been reported in the literature as the anorexigenic effect of Cd. Therefore, Cd increased in plasma, accumulating in the pancreas and in the islets of Langerhans of time-dependent exposed rats (Fig. 1A–C). In serum, Cd can be distributed and exposed to the pancreas, such as complexes Cd-MT, Cd-microglobulins, Cd-albumin, and Cd-transferrin, as reviewed in [32]. Then, Cd uptake and accumulation can be through Ca^{2+} channels, transient receptor potential channels, and solute carriers such as divalent metal transporter 1, zinc transporter proteins, zinc-iron permease, and organic cation transporters as reviewed in [10, 33]. Although the pancreas, and particularly islets of Langerhans, are not the primary target tissues of Cd accumulation, such as the liver and kidney [2, 5], our data showed a significant accumulation, which correlates with previous reports [6]. Wong et al. also informed serum Cd increase and accumulation of the metal in islets of Langerhans from mice exposed to 56.2 ppm in drinking water by 11 weeks [34].

In addition, hyperglycemia and hyperinsulinemia also were observed in Cd-exposed rats (Table 1). Experimental short-term and long-term *in vivo* Cd exposure models have shown hyperglycemia [6, 35, 36]. In the same way, epidemiological studies of subjects with occupational exposure to Cd showed a predisposition to developing hyperglycemia, prediabetes, and diabetes caused by significantly low fasting serum insulin levels, although discrepancies, contradictory, and inconsistent findings exist because the population is not exposed to a one of a kind, at the same time or type of exposure [34, 37–39]. *In vitro*, Cd accumulates within human pancreatic β-cells and alters glucose-stimulated insulin release [35, 36, 40–42]. However, evidence suggests that chronic low-level exposure to Cd in the environment, such as LOAEL dosage, has also been associated with an increased risk of developing dysglycemia and diabetes [5, 6, 10]. Still, it is unrelated to β-cell death [34, 43], despite Cd accumulation and hyperglycemia being stressors for β-cells. This fact is supported by our results that showed a high insulin concentration in islets of Langerhans isolated from groups exposed to Cd and a high immunoreactivity to hormones (Fig. 2A, B). The sustained hyperfunction of β-cells can alter their capacity to downregulate the insulin secretion rate for a long time, as we observed at 3 and 4 months of Cd exposure [44, 45]. Additionally, some ex vivo studies have shown that the accumulation of Cd at environmental levels leads to impaired β-cell function [39, 42]. However, experiments with immortalized murine β-cell line (MIN6) did not show any differences in the ex vivo or in vivo function of intact islets following Cd accumulation, which could be related to their protective defense [34].

The mechanisms associated with cadmium toxicity involve essential biometal competition, disruption of cell signaling pathways, and DNA damage mainly by oxidative stress as reviewed in [10]. Although Cd does not induce oxidative stress directly because it does not possess redox chemistry, it can provoke Fenton and Haber-Weiss reactions, which produce hydroxyl (•OH) and superoxide ($O_2^{\bullet-}$) radicals. Cd also increases ROS through different mitochondrial complexes, which forms excessive ROS and $O_2^{\bullet-}$ [46–48]. Cd also can overinduce NADPH oxidase activity, producing higher ROS and free radical levels. NADPH-dependent ROS production has been described in the liver, kidney, neuronal cells, and multiple Cd-exposed cancer cell lines [49–52]. The over-ROS output of more than the tolerable threshold in

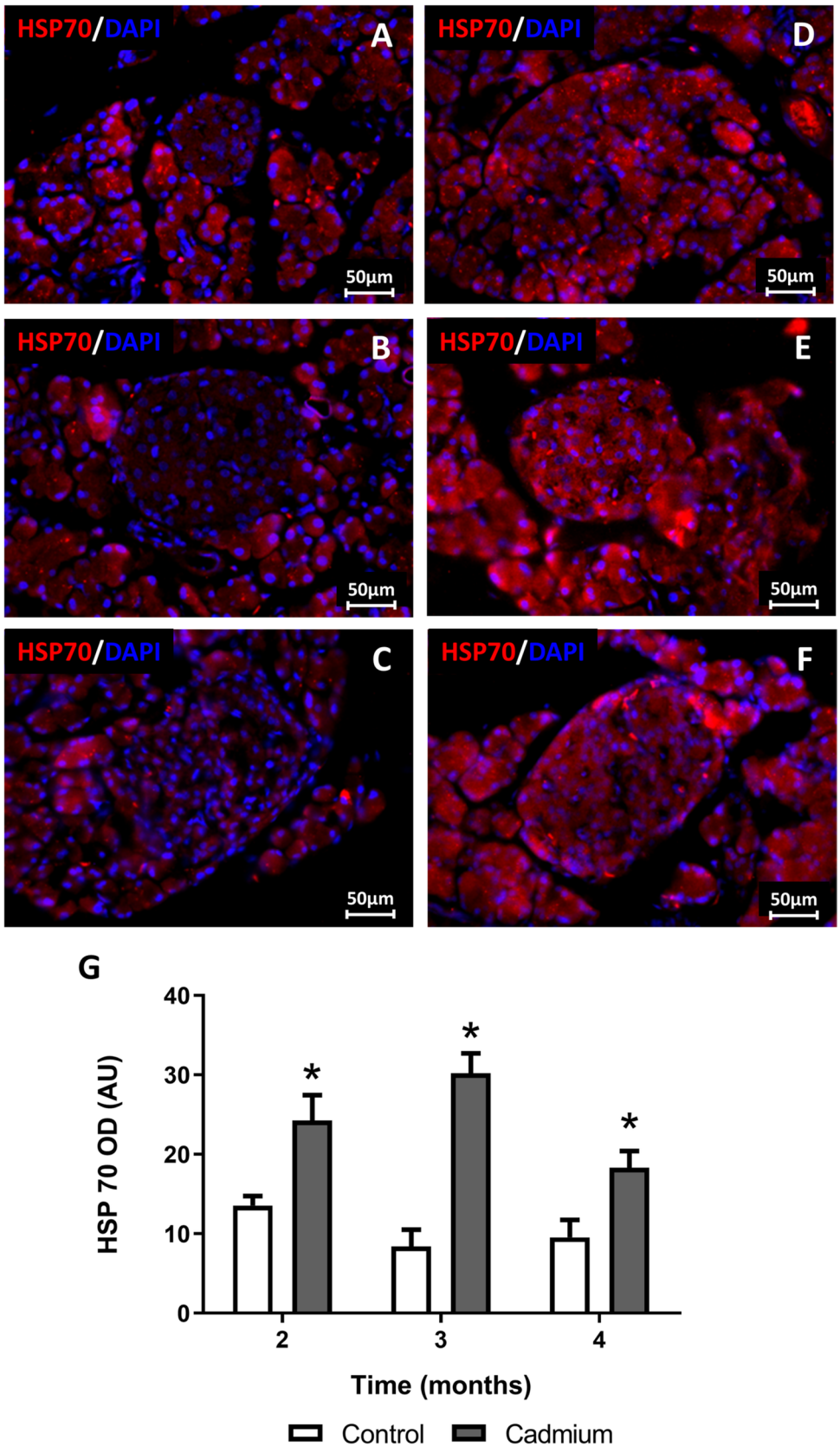

Fig. 5 Heat shock protein 70 analysis. **A–C** Representative photomicrographs of the control groups of 2, 3, and 4 months ($n = 100$ islets; 40× objective). **D–F** Representative photomicrographs of Cd-exposed groups at 2, 3, and 4 months ($n = 100$ islets; 40× objective). **G** Semi-quantitative analysis of the immunoreactivity to HSF1. *Significant difference from the control group ($p \leq 0.05$ by Mann–Whitney U test). The analysis was performed from a delimited area corresponding to Langerhans islets

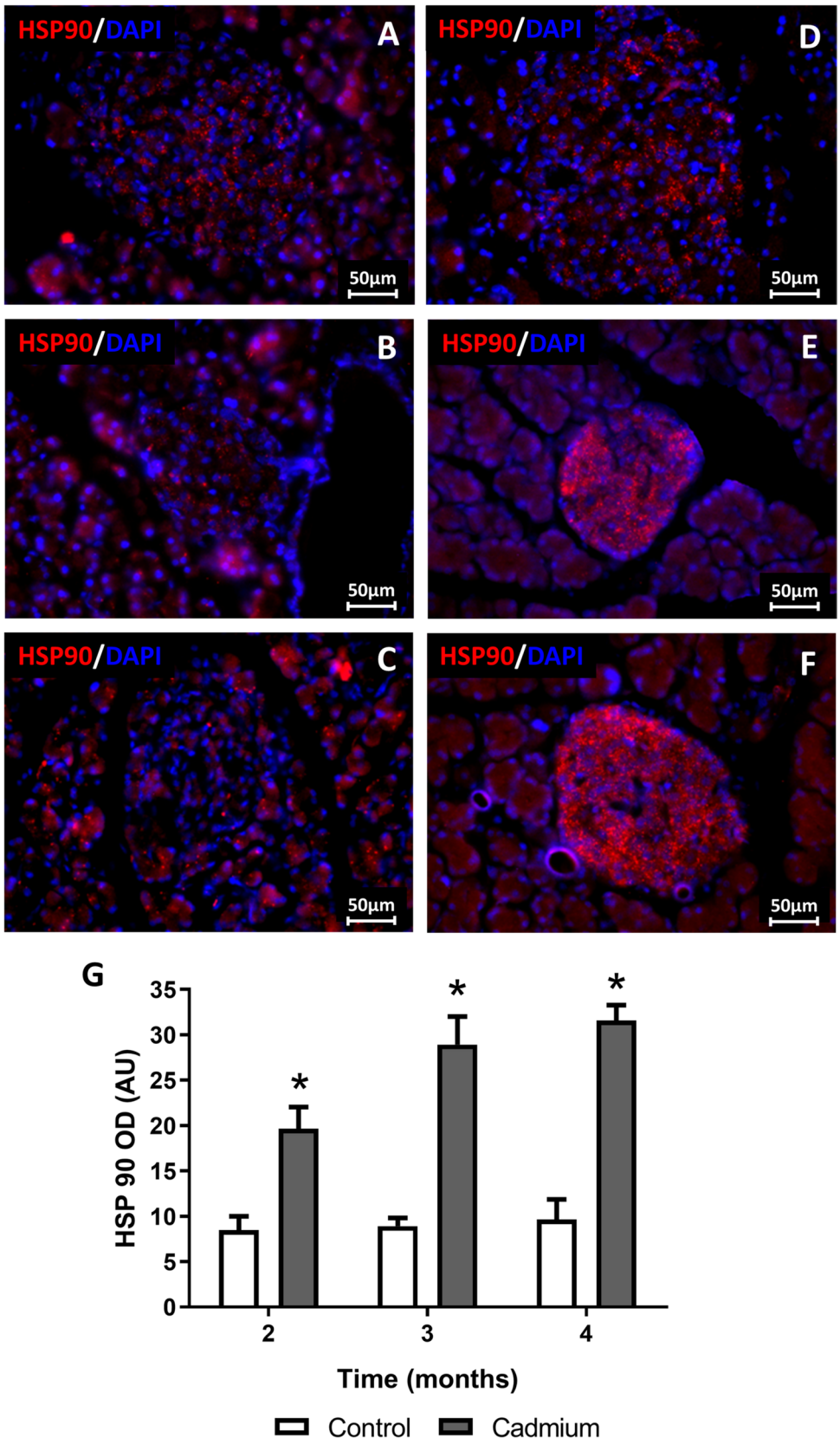

Fig. 6 Heat shock protein 90 analysis. **A–C** Representative photomicrographs of the control groups of 2, 3, and 4 months ($n = 100$ islets; 40× objective). **D–F** Representative photomicrographs of Cd-exposed groups at 2, 3, and 4 months ($n = 100$ islets; 40× objective). **G** Semi-quantitative analysis of the immunoreactivity to HSF1. *Significant difference from the control group ($p \leq 0.05$ by Mann–Whitney U test). The analysis was performed from a delimited area corresponding to Langerhans islets

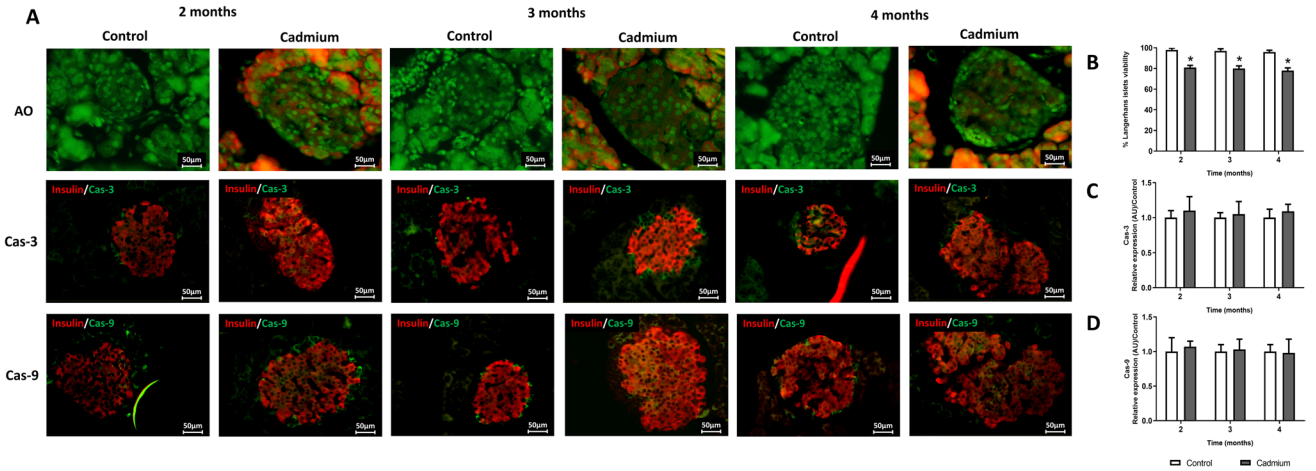

Fig. 7 Viability of Islets of Langerhans and Cas3 and Cas9 with insulin co-expression. Representative photomicrographs of the control and Cd-exposed groups at 2, 3, and 4 months ($n = 100$, islets analyzed). First row acridine orange; second row caspase 3 (green)/insulin (red); and third row caspase 9 (green)/insulin (red). The images were acquired with a 40× objective. **A** Percentage of cell viability. Comparisons between groups were made by Student's "*t*"-test. *Significant difference from the control group ($p \leq 0.05$ by Mann–Whitney *U* test). The analysis was performed from a delimited area corresponding to Langerhans islets

pancreatic cells might lead to membrane lipid peroxidation, mtDNA cleavage, and impaired ATP generation, resulting in cell death [53, 54]. Our results showed a significant ROS increase from 3 months and lipid peroxidation (4HDA and MDA) from 2 months of Cd exposure (Fig. 3A, C, D).

On the other hand, pancreatic antioxidative defense by GSH and MT showed substantial increases from 2 months of Cd exposure (Table 2). However, these were measured in total pancreatic homogenates. MT and GSH have been proposed as primary cell defense; however, MT antioxidant activity is about 50 times higher against oxidative DNA damage and 10 times higher against lipid peroxidation than GSH [13]. It has been reported that Cd exposure to β-cell line MIN6 increases MT1 and MT2 protein levels [55]. Besides metals, MT gene expression in pancreatic cells is also regulated by glucose level, observing high protein expression in hyperglycemic conditions [56–60]. Moreover, islets of Langerhans from rats exposed to H_2O_2, IL-1β, TNF-α, and IFN-γ overexpress MT1 isoform compared to MT2 isoform [60, 61]. Likewise, GSH can bind Cd, ROS, RNS, lipid peroxides, and oxidized DNA to avoid cell damage, both in acinar cells and islets of Langerhans. Cadmium can bind to GSH in equimolar conditions of 1:2 or 1:1 (GS-Cd-GS and GS-Cd). Meanwhile, the GS-Cd-GS complex can be released from cells to diminish Cd concentration; the GS-Cd complex can exchange the metal with MTs, modifying the storage and simultaneously reducing protein damage and cell death. Initially, there is a decrease in GSH levels in response to Cd exposure, whether from Cd–GSH interaction or, more likely, increased oxidative stress, which can lead to a rebound increase in total glutathione levels [62, 63]. However, we observed the opposite in Cd-exposed groups. At the same time, GSSG increased at 3 and 4 months, although under normal circumstances, the redox ratio (2GSH/GSSG) must be maintained in a range of 20–100, such as in the liver [64]. Our results showed that the redox ratio was maintained in Cd-exposed groups. Nevertheless, a diminishing time dependence can be observed (Table 2).

To maintain GSH levels, the pancreatic cell depends on the GSH *novo* synthesis and GSH recycling. GSH recycling is regulated by GR and GST activity. Our results showed that while GST activity increased on time dependence to Cd exposure, GR activity was maintained until 3 months of Cd exposure, diminishing in the fourth month (Table 2). These enzymes are seldom studied in the pancreas, and there are a few reports about their behavior in this tissue with controversial results. Some results showed that GR and GST activities did not change in streptozotocin-treated rats, while others mentioned that their activities decreased [65, 66]. Meanwhile, there is no information on chronic Cd exposure and the activities of these enzymes in the pancreas. It is possible to hypothesize that Cd could affect the flavin adenine dinucleotide site of GR or the enzyme structure, as shown by Bandyopadhyay et al. [67]. This could explain the enzyme activity diminishing because analytical assays provide NADPH, which discards the idea of cofactor exhaustion. On the other hand, the high GST activity could be explained by the need for pancreatic cells to form complexes of GSH with free radicals, ROS, 4HDA, MDA, or Cd to avoid cell damage.

Moreover, in the pancreas, it is reported that GPx has a broader protective spectrum than CAT because, in addition to H_2O_2, it also metabolizes other hydroperoxides, including lipid hydroperoxide, in diabetic rats [66, 68]. Whereas

CAT activity is in the peroxisomes, cytoplasm, nucleus, and mitochondria as reviewed in [69, 70], the cytoplasmic and mitochondrial H_2O_2 detoxification is carried out by GPx isoforms via GSH oxidation [71, 72]. According to the literature, CAT activity is better for severe stress situations as reviewed in [73, 74], while GPx isoforms act better against low levels of H_2O_2. Both rodent and human islets of Langerhans have reduced expression of GPx in physiological conditions that protect β-cells against oxidative stress; thereby, stressors such as hyperglycemia, free radicals, and Cd would involve overexpression and activity of GPx [75, 76]. Our results showed that GPx activity in pancreatic homogenates increased from 2 months of cadmium exposure but significantly decreased at 4 months of metal exposure (Table 2). Contrarily, CAT activity was increased over time, which agrees with ROS levels shown by Cd groups. In addition, pancreatic cells are only equipped with about 50% of SOD, 15% of GPx, and 5% of CAT compared to the liver and muscle [77, 78]. Most studies agree that in high oxidative stress conditions, such as diabetes, hyperglycemia, dyslipidemia, and Cd accumulation, SOD activity increases. Our results confirmed that pancreatic SOD activity increased over time. SOD catalyzes the dismutation of superoxide ($O_2^{\bullet-}$) radical to hydrogen peroxide (H_2O_2); due to high expression in the pancreas, SOD activity prevents harm [79], although its overexpression also is related to cell damage [80]. Total SOD activity during Cd exposure has been studied intensively, and both increases and decreases have been described in the literature [81, 82]. These discrepancies can be attributed to different exposure conditions, the organ studied, and specific isoforms localized in the cell compartments. SODs are classified according to their metal cofactor, cytosolic isoform (CuZnSOD), and mitochondrial isoform (MnSOD) [83, 84]. Temporarily, Cd can inhibit CuZnSOD at both protein and catalytic levels, because Cd-enzyme interaction causes perturbations in the enzyme topography and zinc displacement [85]. The overall MnSOD activity decrease was also informed after Cd exposure [54, 86]. Therefore, SOD and CAT behavior provides evidence of protection for pancreatic parenchyma in highly stressful conditions.

Additionally, in islets of Langerhans, the HSPs are among the most effective defense mechanisms in response to chronic Cd exposure and other stressors such as hyperglycemia. Thus, an HSP upregulation in T2D subjects has been informed, as reviewed in [87]. Likewise, the downregulation of HSP correlates with dysfunction in islets of Langerhans and β-cells [88]. The p-HSF1 translocates to the nucleus, upregulating the gene expression of HSP [89, 90]. Therefore, a high HSF1 expression protects against cell damage, while its impaired expression makes pancreatic cells and islets of Langerhans more susceptible to damage. Our results showed a high HSF1, HSP70, and HSP90 immunoreactivity over time in Cd-exposed groups (Figs. 4, 5, and 6D–G). HSP70 promotes the removal of damaged proteins, and its increases lead to a higher Cd tolerance threshold as reviewed in [91]. In β-cell cultures and pancreas biopsies from T2D subjects, HSP70 avoids islet cell death. Therefore, HSP70 is the major countermeasure against Cd toxicity because it is highly sensitive to environmental assaults [17, 92]. Changes in the concentration of HSP70 can be used as a possible bioindicator and molecular biomarker that can detect Cd intoxication during a LOAEL dose and ROS overgeneration caused by hyperglycemia. Meanwhile, the HSP90 chaperone complexes located in the cytoplasm, endoplasmic reticulum, and mitochondria facilitate the maturation of client proteins as reviewed in [93]. Initially recognized as a stress-induced protein, HSP90 has now been identified as a crucial oncogenic modulator critical for avoiding cancer cell growth and proliferation [19, 94]. In chronic Cd exposure, HSP90 overexpression has been reported in multiple tissues, suggesting a protective tumorigenic role. HSP90 protects islets of Langerhans against hyperglycemia effects in diabetic db/db mice and improves insulin sensitivity in the diet-induced obese mouse model of insulin resistance [20]. HSP90 expression decreases in isolated rat islets exposed to high glucose, affecting glycolysis, ATP generation, and calcium signaling. This suggests that a fine control between oxidative stress and HSP90 expression is mandatory for β-cells [95, 96]. Our results suggest that HSP increased expression could be an additional protection mechanism for the islet of Langerhans in adverse environments such as Cd exposure.

Finally, the HSP70 family inhibits downstream caspase activation and cytochrome c release from mitochondria, counteracting the apoptotic cascade as reviewed in [90]. The apoptotic mechanism follows two pathways, the intrinsic and the extrinsic. For both intrinsic and extrinsic pathways, the ultimate executors of apoptosis are proteases, called caspases, which are activated enzymatically in response to an apoptotic stimulus as reviewed in [97]. Due to their cytoprotective role, HSP has been found to play highly complex functions in regulating apoptosis [98, 99]. They are implicated in both caspase-dependent and independent apoptotic pathways and in the maintenance and activation of antiapoptotic mediators. HSP70 and HSP90 overexpression in the human pancreas plays a master regulatory role in the inhibition or neutralization of pancreatic apoptosis by imparting TNF-related apoptosis-inducing ligand resistance [99], preventing BAX translocation into mitochondria [100], inhibiting caspase-9 recruitment and apoptosome formation as reviewed in [98, 101], providing lysosomal and mitochondrial integrity [102, 103], and suppressing JNK activation and JNK-mediated cell death [104, 105]. Moreover, HSP90 positively regulates Nf-kB and leads to cell survival through PI3K-Akt signaling cascades [106]. Our

results showed undetectable immunoreactivity to caspases 3 and 9 and a high survival percentage in islets of Langerhans cells (Fig. 7).

In summary, chronic Cd exposure at the LOAEL dose causes a serum increase and accumulation of the metal in the pancreas and islets of Langerhans on time dependence. However, it is important to consider that the lower weight in Cd-exposed rats may influence insulin sensitivity. Moreover, Cd-exposed rats develop hyperglycemia and hyperinsulinemia, associated with high insulin production. Although Cd accumulation has been related to oxidative stress, as observed in our results, it did not exceed the damage threshold due to an efficient antioxidative defense by pancreatic parenchyma. An augment in MT and GSH concentrations with the increased enzymatic activity of the glutathione system, catalase, and superoxide dismutase from pancreatic lysates maintained a favorable redox environment, which is probably extensive for islets of Langerhans. However, this fact must be explored in the islets of Langerhans to understand the role of antioxidative defense in the pancreas exocrine. Additionally, islets of Langerhans showed a high immunoreactivity of HSF1, HSP70, and HSP90, which suggests a major protein expression of these proteins that cooperate in cell defense to avoid cell death. The results also showed minimal immunoreactivity to caspases 3 and 9 associated with a high survival rate of islets of Langerhans cells. In conclusion, antioxidative and HSP pancreatic defense avoids cell death associated with Cd accumulation in chronic conditions; however, this could provoke oversynthesis and insulin release, which is a sign of insulin resistance.

Supplementary Information The online version contains supplementary material available at https://doi.org/10.1007/s12011-023-03955-y.

Acknowledgements The authors thank Dr. Francisco Ramos Collazo (Bioterio "Claude Bernard," BUAP) for his assistance and the donation of the animals used in this work. We also express our gratitude to Dra. Yhisell Domínguez Alonso of the Clinical Laboratory "CAISS S.A de C.V" for providing the facilities to carry out this study.

Author Contribution Diana Moroni-González, Eduardo Brambila, and Samuel Treviño designed the study and wrote the protocol. Victor Enrique Sarmiento-Ortega, Alfonso Díaz, Diana Moroni-González, and Samuel Treviño performed the experiments. Diana Moroni-González, Eduardo Brambila, and Samuel Treviño managed the literature searches and analysis. Eduardo Brambila, and Diana Moroni-González carried out the statistical analysis. Diana Moroni-González, Alfonso Díaz, Eduardo Brambila, and Samuel Treviño wrote the first draft of the manuscript. All contributing authors have approved the final manuscript.

Funding The authors thank Vicerrectoria de Investigación y Posgrado [VIEP; TRMS-NAT23] through Ygnacio Martínez Laguna, CONAHCYT, and the "Sistema Nacional de Investigadores" of Mexico for the financial support of this research project [DMG, 758984].

Declarations

Competing Interests The authors report no conflicts of interest.

References

1. ATSDR (2012) Toxicological profile for cadmium. Agency for Toxic Substances and Disease Registry, Public Health Service-US Department of Health and Human Services, pp 1–487
2. Lee WK, Thévenod F (2020) Cell organelles as targets of mammalian cadmium toxicity. Arch Toxicol 94:1017–1049. https://doi.org/10.1007/S00204-020-02692-8
3. Satarug S, Nishijo M, Ujjin P, Moore MR (2018) Chronic exposure to low-level cadmium induced zinc-copper dysregulation. J Trace Elem Med Biol 46:32–38. https://doi.org/10.1016/j.jtemb.2017.11.008
4. Sarmiento-Ortega VE, Moroni-González D, Diaz A et al (2022) ROS and ERK pathway mechanistic approach on hepatic insulin resistance after chronic oral exposure to cadmium NOAEL dose. Biol Trace Elem Res 1–16. https://doi.org/10.1007/S12011-022-03471-5/FIGURES/3
5. Sarmiento-Ortega VE, Moroni-González D, Díaz A et al (2021) Oral subacute exposure to cadmium LOAEL dose induces insulin resistance and impairment of the hormonal and metabolic liver-adipose axis in Wistar rats. Biol Trace Elem Res. https://doi.org/10.1007/S12011-021-03027-Z
6. Treviño S, Waalkes MP, Flores Hernández JA et al (2015) Chronic cadmium exposure in rats produces pancreatic impairment and insulin resistance in multiple peripheral tissues. Arch Biochem Biophys 583:27–35. https://doi.org/10.1016/j.abb.2015.07.010
7. Santamaria-Juarez C, Atonal-Flores F, Diaz A et al (2020) Aortic dysfunction by chronic cadmium exposure is linked to multiple metabolic risk factors that converge in anion superoxide production. Arch Physiol Biochem 1–9. https://doi.org/10.1080/13813455.2020.1726403
8. Treviño S, Pulido G, Fuentes E et al (2022) Effect of cadmium administration on the antioxidant system and neuronal death in the hippocampus of rats. Synapse 76:e22242. https://doi.org/10.1002/SYN.22242
9. Sarmiento-Ortega VE, Treviño S, Flores-Hernández JÁ et al (2017) Changes on serum and hepatic lipidome after a chronic cadmium exposure in Wistar rats. Arch Biochem Biophys 635:52–59. https://doi.org/10.1016/j.abb.2017.10.003
10. Moroni-González D, Sarmiento-Ortega VE, Diaz A et al (2023) Pancreas–liver–adipose axis: target of environmental cadmium exposure linked to metabolic diseases. Toxics 223(11):223. https://doi.org/10.3390/TOXICS11030223
11. Ježek P, Holendová B, Jabůrek M et al (2021) The pancreatic β-cell: the perfect redox system. Antioxidants 10:1–64. https://doi.org/10.3390/ANTIOX10020197
12. Halliwell B (2006) Reactive species and antioxidants. Redox biology is a fundamental theme of aerobic life. Plant Physiol 141:312. https://doi.org/10.1104/PP.106.077073
13. Miura T, Muraoka S, Ogiso T (1997) Antioxidant activity of metallothionein compared with reduced glutathione. Life Sci 60:301–309. https://doi.org/10.1016/S0024-3205(97)00156-2
14. Alnahdi A, John A, Raza H (2019) N-acetyl cysteine attenuates oxidative stress and glutathione-dependent redox imbalance caused by high glucose/high palmitic acid treatment in pancreatic Rin-5F cells. PLoS One 14. https://doi.org/10.1371/JOURNAL.PONE.0226696
15. Sabolić I, Breljak D, Škarica M, Herak-Kramberger CM (2010) Role of metallothionein in cadmium traffic and toxicity in kidneys and other mammalian organs. BioMetals 23:897–926. https://doi.org/10.1007/S10534-010-9351-Z
16. Krause M, Bock PM, Takahashi HK et al (2015) The regulatory roles of NADPH oxidase, intra-and extra-cellular HSP70

in pancreatic islet function, dysfunction and diabetes. Clin Sci 128:789–803. https://doi.org/10.1042/CS20140695
17. Marina Piscopo NR, Piscopo M TJ (2017) hsp70 as new cadmium bioaccumulation marker to prevent the risks of mussels consumption in human nutrition. Madridge J Clin Res 2:39–35. https://doi.org/10.18689/MJCR-1000107
18. Radons J (2016) The human HSP70 family of chaperones: where do we stand? Cell Stress Chaperones 21:379. https://doi.org/10.1007/S12192-016-0676-6
19. Zhu K, Zhang Y, Zhang J et al (2020) Acetylation of Hsp90 reverses dexamethasone-mediated inhibition of insulin secretion. Toxicol Lett 320:19–27. https://doi.org/10.1016/j.toxlet.2019.11.022
20. Yang X, Zhang Y, Xu W et al (2016) Potential role of Hsp90 in rat islet function under the condition of high glucose. Acta Diabetol 53:621–628. https://doi.org/10.1007/s00592-016-0852-2
21. McCall MD, Maciver AH, Pawlick R et al (2011) Histopaque provides optimal mouse islet purification kinetics: comparison study with Ficoll, iodixanol and dextran. Islets 3:144–149. https://doi.org/10.4161/ISL.3.4.15729
22. Sánchez-Solís CN, Hernández-Fragoso H, Aburto-Luna V et al (2021) Kidney adaptations prevent loss of trace elements in Wistar rats with early metabolic syndrome. Biol Trace Elem Res 199:1941–1953. https://doi.org/10.1007/S12011-020-02317-2
23. Sedmak JJ, Grossberg SE (1977) A rapid, sensitive, and versatile assay for protein using Coomassie brilliant blue G250. Anal Biochem 79:544–552. https://doi.org/10.1016/0003-2697(77)90428-6
24. Erdelmeier I, Gérard-Monnier D, Régnard K et al (1998) Reactions of 1-methyl-2-phenylindole with malondialdehyde and 4-hydroxyalkenals. Analytical applications to a colorimetric assay of lipid peroxidation. Chem Res Toxicol 11:1176–1183. https://doi.org/10.1021/TX9701790
25. Tsikas D (2007) Analysis of nitrite and nitrate in biological fluids by assays based on the Griess reaction: appraisal of the Griess reaction in the L-arginine/nitric oxide area of research. J Chromatogr B Analyt Technol Biomed Life Sci 851:51–70. https://doi.org/10.1016/J.JCHROMB.2006.07.054
26. Eaton DL, George Cherian M (1991) Determination of metallothionein in tissues by cadmium-hemoglobin affinity assay. Methods Enzymol 205:83–88. https://doi.org/10.1016/0076-6879(91)05089-E
27. Rahman I, Kode A, Biswas SK (2006) Assay for quantitative determination of glutathione and glutathione disulfide levels using enzymatic recycling method. Nat Protoc 1:3159–3165. https://doi.org/10.1038/NPROT.2006.378
28. Flohé L, Günzler WA (1984) Assays of glutathione peroxidase. Methods Enzymol 105:114–120. https://doi.org/10.1016/S0076-6879(84)05015-1
29. Habig WH, Pabst MJ, Jakoby WB (1974) Glutathione S-transferases. The first enzymatic step in mercapturic acid formation. J Biol Chem 249:7130–7139
30. Smith IK, Vierheller TL, Thorne CA (1988) Assay of glutathione reductase in crude tissue homogenates using 5,5'-dithiobis(2-nitrobenzoic acid). Anal Biochem 175:408–413. https://doi.org/10.1016/0003-2697(88)90564-7
31. Aebi H (1984) Catalase in vitro. Methods Enzymol 105:121–126. https://doi.org/10.1016/S0076-6879(84)05016-3
32. Freisinger E, Vašák M (2013) Cadmium in metallothioneins. Met Ions Life Sci 11:339–371. https://doi.org/10.1007/978-94-007-5179-8_11
33. Thévenod F, Fels J, Lee W-K, Zarbock R (2019) Channels, transporters and receptors for cadmium and cadmium complexes in eukaryotic cells: myths and facts. BioMetals. https://doi.org/10.1007/s10534-019-00176-6
34. Wong WPS, Wang JC, Meyers MS et al (2022) A novel chronic in vivo oral cadmium exposure-washout mouse model for studying cadmium toxicity and complex diabetogenic effects. Toxicol Appl Pharmacol 447:116057–116057. https://doi.org/10.1016/J.TAAP.2022.116057
35. Edwards J, Ackerman C (2016) A review of diabetes mellitus and exposure to the environmental toxicant cadmium with an emphasis on likely mechanisms of action. Curr Diabetes Rev 12:252–258. https://doi.org/10.2174/1573399811666150812142922
36. Fitzgerald R, Olsen A, Nguyen J et al (2021) Pancreatic islets accumulate cadmium in a rodent model of cadmium-induced hyperglycemia. Int J Mol Sci 22:1–16. https://doi.org/10.3390/IJMS22010360
37. Barregard L, Bergström G, Fagerberg B (2013) Cadmium exposure in relation to insulin production, insulin sensitivity and type 2 diabetes: a cross-sectional and prospective study in women. Environ Res 121:104–109. https://doi.org/10.1016/J.ENVRES.2012.11.005
38. Borné Y, Fagerberg B, Persson M et al (2014) Cadmium exposure and incidence of diabetes mellitus - results from the Malmö Diet and Cancer study. PLoS One 9. https://doi.org/10.1371/JOURNAL.PONE.0112277
39. Wong WP, Allen NB, Meyers MS et al (2017) Exploring the association between demographics, SLC30A8 genotype, and human islet content of zinc, cadmium, copper, iron, manganese and nickel. Sci Rep 7. https://doi.org/10.1038/S41598-017-00394-3
40. Fatima G, Raza AM, Hadi N et al (2019) Cadmium in human diseases: it's more than just a mere metal. Indian J Clin Biochem 34:371–378
41. Lei L, Jin T, YF Z (2007) Insulin expression in rats exposed to cadmium - PubMed. Biomed Environ Sci 20:295–301
42. El MM, Raja MR, Zhang X et al (2012) Accumulation of cadmium in insulin-producing β cells. Islets 4:405. https://doi.org/10.4161/ISL.23101
43. Moulis J-M, Thévenod F (2010) New perspectives in cadmium toxicity: an introduction. BioMetals 23:763–768. https://doi.org/10.1007/s10534-010-9365-6
44. Paschen M, Moede T, Valladolid-Acebes I et al (2019) Diet-induced β-cell insulin resistance results in reversible loss of functional β-cell mass. FASEB J 33:204–218. https://doi.org/10.1096/fj.201800826R
45. Shanik MH, Xu Y, Škrha J et al (2008) Insulin resistance and hyperinsulinemia. Diabetes Care 31:S262–S268. https://doi.org/10.2337/dc08-s264
46. Branca JJV, Morucci G, Maresca M et al (2018) Selenium and zinc: two key players against cadmium-induced neuronal toxicity. Toxicol In Vitro 48:159–169. https://doi.org/10.1016/J.TIV.2018.01.007
47. Branca JJV, Morucci G, Becatti M et al (2019) Cannabidiol protects dopaminergic neuronal cells from cadmium. Int J Environ Res Public Health 16. https://doi.org/10.3390/IJERPH16224420
48. Branca JJV, Pacini A, Gulisano M et al (2020) Cadmium-induced cytotoxicity: effects on mitochondrial electron transport chain. Front Cell Dev Biol 8:604377. https://doi.org/10.3389/FCELL.2020.604377/BIBTEX
49. El-kott AF, Alshehri AS, Khalifa HS et al (2020) Cadmium chloride induces memory deficits and hippocampal damage by activating the JNK/p66Shc/NADPH oxidase axis. Int J Toxicol 39:477–490. https://doi.org/10.1177/1091581820930651
50. Mohammadi-Bardbori A, Rannug A (2014) Arsenic, cadmium, mercury and nickel stimulate cell growth via NADPH oxidase activation. Chem Biol Interact 224:183–188. https://doi.org/10.1016/J.CBI.2014.10.034
51. Gupta DK, Pena LB, Romero-Puertas MC et al (2017) NADPH oxidases differentially regulate ROS metabolism and nutrient

uptake under cadmium toxicity. Plant Cell Environ 40:509–526. https://doi.org/10.1111/PCE.12711
52. Souza V, del Escobar MC, Bucio L et al (2009) NADPH oxidase and ERK1/2 are involved in cadmium induced-STAT3 activation in HepG2 cells. Toxicol Lett 187:180–186. https://doi.org/10.1016/J.TOXLET.2009.02.021
53. Souza V, Flores K, Ortiz L et al (2012) Liver and cadmium toxicity. J Drug Metab Toxicol 5:5. https://doi.org/10.4172/2157-7609.S5-001
54. Jihen EH, Imed M, Fatima H, Abdelhamid K (2009) Protective effects of selenium (Se) and zinc (Zn) on cadmium (Cd) toxicity in the liver of the rat: effects on the oxidative stress. Ecotoxicol Environ Saf 72:1559–1564. https://doi.org/10.1016/J.ECOENV.2008.12.006
55. El Muayed M, Raja MR, Zhang X et al (2012) Accumulation of cadmium in insulin-producing β cells. Islets 4:405–416. https://doi.org/10.4161/isl.23101
56. Bellomo E, Meur G, Rutter G (2011) Glucose regulates free cytosolic Zn^{2+} concentration, Slc39 (ZiP), and metallothionein gene expression in primary pancreatic islet β-cells. J Biol Chem 286:25778–25789. https://doi.org/10.1074/JBC.M111.246082
57. Zimny S, Gogolin F, Abel J, Gleichmann H (1993) Metallothionein in isolated pancreatic islets of mice: induction by zinc and streptozotocin, a naturally occurring diabetogen. Arch Toxicol 67:61–65. https://doi.org/10.1007/BF02072037
58. Ohly P, Dohle C, Abel J et al (2000) Zinc sulphate induces metallothionein in pancreatic islets of mice and protects against diabetes induced by multiple low doses of streptozotocin. Diabetologia 43:1020–1030. https://doi.org/10.1007/S001250050009
59. Duprez J, Roma L, Close A, Jonas J (2012) Protective antioxidant and antiapoptotic effects of ZnCl2 in rat pancreatic islets cultured in low and high glucose concentrations. PLoS One 7. https://doi.org/10.1371/JOURNAL.PONE.0046831
60. Jonas JC, Bensellam M, Duprez J et al (2009) Glucose regulation of islet stress responses and β-cell failure in type 2 diabetes. Diabetes Obes Metab 11:65–81. https://doi.org/10.1111/j.1463-1326.2009.01112.x
61. Bensellam M, Laybutt DR, Jonas J-C (2021) Emerging roles of metallothioneins in beta cell pathophysiology: beyond and above metal homeostasis and antioxidant response. Biology (Basel) 10:176. https://doi.org/10.3390/BIOLOGY10030176
62. Adamis PDB, Mannarino SC, Eleutherio ECA (2009) Glutathione and gamma-glutamyl transferases are involved in the formation of cadmium–glutathione complex. FEBS Lett 583:1489–1492. https://doi.org/10.1016/J.FEBSLET.2009.03.066
63. Pearson SA, Cowan JA (2021) Glutathione-coordinated metal complexes as substrates for cellular transporters. Metallomics 13:15. https://doi.org/10.1093/MTOMCS/MFAB015
64. Delalande O, Desvaux H, Godat E et al (2010) Cadmium - glutathione solution structures provide new insights into heavy metal detoxification. FEBS J 277:5086–5096. https://doi.org/10.1111/J.1742-4658.2010.07913.X
65. Gok M, Ulusu NN, Tarhan N et al (2016) Flaxseed protects against diabetes-induced glucotoxicity by modulating pentose phosphate pathway and glutathione-dependent enzyme activities in rats. J Diet Suppl 13:339–351. https://doi.org/10.3109/19390211.2015.1036188
66. Erejuwa OO, Sulaiman SA, Wahab MSA et al (2010) Antioxidant protective effect of glibenclamide and metformin in combination with honey in pancreas of streptozotocin-induced diabetic rats. Int J Mol Sci 11(11):2056–2066. https://doi.org/10.3390/IJMS11052056
67. Bandyopadhyay D, Chatterjee AK, Datta AG (1993) Effect of cadmium treatment on hepatic flavin metabolism. J Nutr Biochem 4:510–514. https://doi.org/10.1016/0955-2863(93)90086-C
68. Pădureanu V, Florescu DN, Pădureanu R et al (2022) Role of antioxidants and oxidative stress in the evolution of acute pancreatitis (review). Exp Ther Med 23. https://doi.org/10.3892/ETM.2022.11120
69. Glorieux C, Calderon P (2017) Catalase, a remarkable enzyme: targeting the oldest antioxidant enzyme to find a new cancer treatment approach. Biol Chem 398:1095–1108. https://doi.org/10.1515/HSZ-2017-0131
70. Schrader M, Fahimi H (2004) Mammalian peroxisomes and reactive oxygen species. Histochem Cell Biol 122:383–393. https://doi.org/10.1007/S00418-004-0673-1
71. Kalyanaraman B (2013) Teaching the basics of redox biology to medical and graduate students: oxidants, antioxidants and disease mechanisms. Redox Biol 1:244–257. https://doi.org/10.1016/J.REDOX.2013.01.014
72. Svensson B (1988) Abilities of peroxidases to catalyse peroxidase-oxidase oxidation of thiols. Biochem J 256:757–762. https://doi.org/10.1042/BJ2560757
73. Glorieux C, Zamocky M, Sandoval J et al (2015) Regulation of catalase expression in healthy and cancerous cells. Free Radic Biol Med 87:84–97. https://doi.org/10.1016/J.FREERADBIOMED.2015.06.017
74. Matés JM (2000) Effects of antioxidant enzymes in the molecular control of reactive oxygen species toxicology. Toxicology 153
75. Robertson RP, Harmon JS (2007) Pancreatic islet β-cell and oxidative stress: the importance of glutathione peroxidase. FEBS Lett 581:3743. https://doi.org/10.1016/J.FEBSLET.2007.03.087
76. Ježek P, Jabůrek M, Plecitá-Hlavatá L (2019) Contribution of oxidative stress and impaired biogenesis of pancreatic β-cells to type 2 diabetes. Antioxid Redox Signal 31:722. https://doi.org/10.1089/ARS.2018.7656
77. Lenzen S (2008) Oxidative stress: the vulnerable β-cell. Biochem Soc Trans 36:343–347. https://doi.org/10.1042/BST0360343
78. Grankvist K, Marklund SL, Taljedal IB (1981) CuZn-superoxide dismutase, Mn-superoxide dismutase, catalase and glutathione peroxidase in pancreatic islets and other tissues in the mouse. Biochem J 199:393–398. https://doi.org/10.1042/BJ1990393
79. Islam MN, Rauf A, Fahad FI et al (2022) Superoxide dismutase: an updated review on its health benefits and industrial applications. Crit Rev Food Sci Nutr 62:7282–7300. https://doi.org/10.1080/10408398.2021.1913400
80. Gardner R, Salvador A, Moradas-Ferreira P (2002) Why does SOD overexpression sometimes enhance, sometimes decrease, hydrogen peroxide production? A minimalist explanation. Free Radic Biol Med 32:1351–1357. https://doi.org/10.1016/S0891-5849(02)00861-4
81. Saed-Moucheshi A, Sohrabi F, Fasihfar E et al (2021) Superoxide dismutase (SOD) as a selection criterion for triticale grain yield under drought stress: a comprehensive study on genomics and expression profiling, bioinformatics, heritability, and phenotypic variability. BMC Plant Biol 21. https://doi.org/10.1186/S12870-021-02919-5
82. Wang Y, Branicky R, Noë A, Hekimi S (2018) Superoxide dismutases: dual roles in controlling ROS damage and regulating ROS signaling. J Cell Biol 217:1915–1928. https://doi.org/10.1083/JCB.201708007
83. Bresciani G, da Cruz I, González-Gallego J (2015) Manganese superoxide dismutase and oxidative stress modulation. Adv Clin Chem 68:87–130. https://doi.org/10.1016/BS.ACC.2014.11.001
84. Jurczuk M, Brzóska MM, Moniuszko-Jakoniuk J et al (2004) Antioxidant enzymes activity and lipid peroxidation in liver and kidney of rats exposed to cadmium and ethanol. Food Chem Toxicol 42:429–438. https://doi.org/10.1016/J.FCT.2003.10.005
85. Huang YH, Shih CM, Huang CJ et al (2006) Effects of cadmium on structure and enzymatic activity of Cu,Zn-SOD and oxidative

status in neural cells. J Cell Biochem 98:577–589. https://doi.org/10.1002/JCB.20772
86. Jihen EH, Sonia S, Fatima H et al (2011) Interrelationships between cadmium, zinc and antioxidants in the liver of the rat exposed orally to relatively high doses of cadmium and zinc. Ecotoxicol Environ Saf 74:2099–2104. https://doi.org/10.1016/J.ECOENV.2011.06.008
87. Kondo T, Koga S, Matsuyama R et al (2011) Heat shock response regulates insulin sensitivity and glucose homeostasis: pathophysiological impact and therapeutic potential. Curr Diabetes Rev 7:264–269. https://doi.org/10.2174/157339911796397811
88. McCarty MF (2006) Induction of heat shock proteins may combat insulin resistance. Med Hypotheses 66:527–534. https://doi.org/10.1016/j.mehy.2004.08.033
89. Takeda T, Tsuura Y, Fujita J et al (2001) Heat shock restores insulin secretion after injury by nitric oxide by maintaining glucokinase activity in rat islets. Biochem Biophys Res Commun 284:20–25. https://doi.org/10.1006/bbrc.2001.4933
90. Lanneau D, de Thonel A, Maurel S et al (2007) Apoptosis versus cell differentiation: role of heat shock proteins HSP90, HSP70 and HSP27. Prion 1:53–60. https://doi.org/10.4161/pri.1.1.4059
91. Bimonte VM, Besharat ZM, Antonioni A et al (2021) The endocrine disruptor cadmium: a new player in the pathophysiology of metabolic diseases. J Endocrinol Investig 44:1363–1377. https://doi.org/10.1007/S40618-021-01502-X
92. Han SG, Castranova V, Vallyathan V (2007) Comparative cytotoxicity of cadmium and mercury in a human bronchial epithelial cell line (BEAS-2B) and its role in oxidative stress and induction of heat shock protein 70:852–860. https://doi.org/10.1080/15287390701212695
93. Birbo B, Madu EE, Madu CO et al (2021) Role of HSP90 in cancer. Int J Mol Sci 22:10317. https://doi.org/10.3390/IJMS221910317
94. Graner MW (2016) HSP90 and immune modulation in cancer. Adv Cancer Res 129:191–224. https://doi.org/10.1016/BS.ACR.2015.10.001
95. Lee JH, Gao J, Kosinski PA et al (2013) Heat shock protein 90 (HSP90) inhibitors activate the heat shock factor 1 (HSF1) stress response pathway and improve glucose regulation in diabetic mice. Biochem Biophys Res Commun 430:1109–1113. https://doi.org/10.1016/j.bbrc.2012.12.029
96. Watkins RA, Evans-Molina C, Terrell JK et al (2016) Proinsulin and heat shock protein 90 as biomarkers of beta-cell stress in the early period after onset of type 1 diabetes. Transl Res 168:96–106.e1. https://doi.org/10.1016/j.trsl.2015.08.010
97. Svandova E, Lesot H, Sharpe P, Matalova E (2023) Making the head: caspases in life and death. Front Cell Dev Biol 10:1075751. https://doi.org/10.3389/FCELL.2022.1075751/BIBTEX
98. Ikwegbue PC, Masamba P, Oyinloye BE, Kappo AP (2018) Roles of heat shock proteins in apoptosis, oxidative stress, human inflammatory diseases, and cancer. Pharmaceuticals 11. https://doi.org/10.3390/PH11010002
99. Karabulut S, Gürsoy Gürgen D, Kutlu P, Keskin I (2022) The role of TNF-α and its target HSP-70 in triggering apoptosis in normozoospermic and non-normozoospermic samples. Biopreserv Biobank 20:485–492. https://doi.org/10.1089/BIO.2021.0056
100. Kennedy D, Jäger R, Mosser DD, Samali A (2014) Regulation of apoptosis by heat shock proteins. IUBMB Life 66:327–338. https://doi.org/10.1002/IUB.1274
101. Lanneau D, Brunet M, Frisan E et al (2008) Heat shock proteins: essential proteins for apoptosis regulation. J Cell Mol Med 12:743–761. https://doi.org/10.1111/J.1582-4934.2008.00273.X
102. Havalová H, Ondrovičová G, Keresztesová B et al (2021) Mitochondrial HSP70 chaperone system-the influence of post-translational modifications and involvement in human diseases. Int J Mol Sci 22:8077. https://doi.org/10.3390/IJMS22158077/S1
103. Chine VB, Au NPB, Ma CHE (2019) Therapeutic benefits of maintaining mitochondrial integrity and calcium homeostasis by forced expression of Hsp27 in chemotherapy-induced peripheral neuropathy. Neurobiol Dis 130. https://doi.org/10.1016/J.NBD.2019.104492
104. Kondo T, Sasaki K, Matsuyama R et al (2012) Hyperthermia with mild electrical stimulation protects pancreatic β-cells from cell stresses and apoptosis. Diabetes 61:838–847. https://doi.org/10.2337/DB11-1098
105. Kuppuswami J, Senthilkumar GP (2023) Nutri-stress, mitochondrial dysfunction, and insulin resistance—role of heat shock proteins. Cell Stress Chaperones 28:35. https://doi.org/10.1007/S12192-022-01314-9
106. Shomali N, Marofi F, Tarzi S et al (2021) HSP90 inhibitor modulates HMGA1 and HMGB2 expression along with cell viability via NF-KB signaling pathways in melanoma in-vitro. Gene Rep 24:101205. https://doi.org/10.1016/J.GENREP.2021.101205